ISSN (Print) 1226-1750
ISSN (Online) 2233-6656
Journal of Magnetics 18(4), 395-399 (2013) http://dx.doi.org/10.4283/JMAG.2013.18.4.395

Thermal Stability, Mechanical Properties and Magnetic Properties of Fe-based Amorphous Ribbons with the Addition of Mo and Nb

Bo-Kyeong Han[1], Hye-in Jo[1], Jin Kyu Lee[2], Ki Buem Kim[3], and Haein Yim[1]*

[1]*Department of Physics, Sookmyung Women's University, Seoul 140-742, Korea*
[2]*Div. of Advanced Materials Engineering, Kongju National University, Kongju 314-701, Korea*
[3]*Department of Nanotechnology and Advanced Materials Engineering, Sejong University, Seoul 143-747, Korea*

(Received 1 July 2013, Received in final form 12 September 2013, Accepted 12 September 2013)

The metallic glass ribbons of $[(Fe_xCo_{1-x})_{0.75}B_{0.2}Si_{0.05}]_{96}Mo_4$ (x = 0, 0.3, 0.6, 0.9 at. %) and $[(Fe_xCo_{1-x})_{0.75}B_{0.2}Si_{0.05}]_{96}Nb_4$ (x = 0, 0.3, 0.6, 0.9 at. %) were obtained by melt spinning with 25-30 μm thickness. The thermal stability, mechanical properties and magnetic properties of Fe-Co-B-Si based systems were investigated. The values of thermal stability were measured using differential scanning calorimetry (DSC), including glass transition temperature (T_g), crystallization temperature (T_x) and supercooled liquid region ($\Delta T_x = T_x - T_g$). These amorphous ribbons were identified as fully amorphous, using X-ray diffraction (XRD). The mechanical properties of Fe-based samples were measured by nano-indentation. Magnetic properties of the amorphous ribbons were measured by a vibrating sample magnetometer (VSM). The amorphous ribbons of $[(Fe_xCo_{1-x})_{0.75}B_{0.2}Si_{0.05}]_{96}Mo_4$ (x = 0, 0.3, 0.6, 0.9 at. %) and $[(Fe_xCo_{1-x})_{0.75}B_{0.2}Si_{0.05}]_{96}Nb_4$ (x = 0, 0.3, 0.6, 0.9 at. %) exhibited soft magnetic properties with low coercive force (H_c) and high saturation magnetization (Ms).

Keywords : Fe-based, amorphous, ferromagnetic, soft magnetic properties

1. Introduction

The first amorphous metal was synthesized in 1934 by evaporation method [1]. Since the amorphous phase was first obtained in thin ribbon form metal of Au-Si system through rapid solidification process by Duwez in 1960 [2], various systems of amorphous alloys have been produced. In comparison with crystalline metals, bulk metallic glasses (BMGs) possess high fracture toughness, strength and low plasticity [3-5]. Among these systems of BMGs, F-P-C alloy of Fe-based BMGs was first synthesized in 1967 [6]. Subsequently, Fe-based amorphous alloy systems have attracted interest for the low material cost, ultrahigh strength, high corrosion resistance and good soft magnetic properties [4, 7-10, 17].

Especially, improving the soft magnetic properties and glass forming ability of Fe-based amorphous alloy systems has been studied for the applications of magnetic heads, sensors, magnetic memories and electro magnetic cores [11-13]. For these reasons, Fe-based amorphous alloy systems have become a major topic of BMGs. Of these systems, (Fe,Co)-B-Si alloy system was developed in 1974 and used in application areas for its good soft magnetic properties and high-strength compared with other Fe-B-Si systems [14-16]. As such we have selected [Fe,Co]-B-Si system for this study.

Elements of Mo and Nb were also used as additions to the Fe-B-Si systems, as Mo and Nb enhance glass-forming ability (GFA) and thermal stability. Moreover, these elements do not decrease soft magnetic properties, in contradistinction to B and Si [16].

In this study, we aimed at obtaining Fe-based ferromagnetic BMGs of good soft magnetic properties and high GFA. We studied the effects of replacing Co by Fe and the role of small Mo and Nb additions, using Fe-Co-B-Si-(Mo,Nb) alloy systems. Herein we describe the thermal stability, mechanical properties and magnetic properties of $[(Fe_xCo_{1-x})_{0.75}B_{0.2}Si_{0.05}]_{96}Mo_4$ (x = 0, 0.3, 0.6, 0.9 at. %) and $[(Fe_xCo_{1-x})_{0.75}B_{0.2}Si_{0.05}]_{96}Nb_4$ (x = 0, 0.3, 0.6, 0.9 at. %) of amorphous ribbons in detail.

2. Experimental Procedure

Multi-component ingots (6 g) with the composition of

*Corresponding author: Tel: +82-2-710-9239
Fax: +82-2-2077-7320, e-mail: haein@sookmyung.ac.kr

$[(Fe_xCo_{1-x})_{0.75}B_{0.2}Si_{0.05}]_{96}Mo_4$ (x = 0, 0.3, 0.6, 0.9 at. %) and $[(Fe_xCo_{1-x})_{0.75}B_{0.2}Si_{0.05}]_{96}Nb_4$ (x = 0, 0.3, 0.6, 0.9 at. %) were prepared by an arc-melting furnace with high purity metals, (Fe, Co, B, Mo > 99.95 wt %, Si > 99.999 wt %), under Ti-gettered Argon atmosphere. Each high-purified ingot was melted at least five times under high arc-power for compositional homogenization. From these samples, ribbons with thickness of 25-30 μm and width of 1-3 mm were prepared through single copper roller melt spinning. Glass transition temperature (T_g), crystallization temperature (T_x) and supercooled liquid region ($\Delta T_x = T_x - T_g$) were examined by differential scanning calorimetry (DSC), at a heating rate of 0.67 K/s in room temperature to 700 °C. The structure characteristic was identified using X-ray diffraction (XRD) with Cu-Kα radiation (Cu-Kα, λ = 154050 Å). Also mechanical properties of $[(Fe_xCo_{1-x})_{0.75}B_{0.2}Si_{0.05}]_{96}Mo_4$ (x = 0, 0.3, 0.6, 0.9 at. %) and $[(Fe_xCo_{1-x})_{0.75}B_{0.2}Si_{0.05}]_{96}Nb_4$ (x = 0, 0.3, 0.6, 0.9 at. %) were investigated using nano-indentation experiments with a Berkovich indenter. Nano-indentation test was executed with a maximum load of 50.0 mN, loading rate and unloading rate 100 mN/min. The saturated magnetization (M_s) and coercivity (H_c) of these amorphous ribbons were measured using a vibrating sample magnetometer (VSM) at room temperature. These amorphous ribbons were examined by in-plane magnetic field of range −1.0 G to 1.0 G.

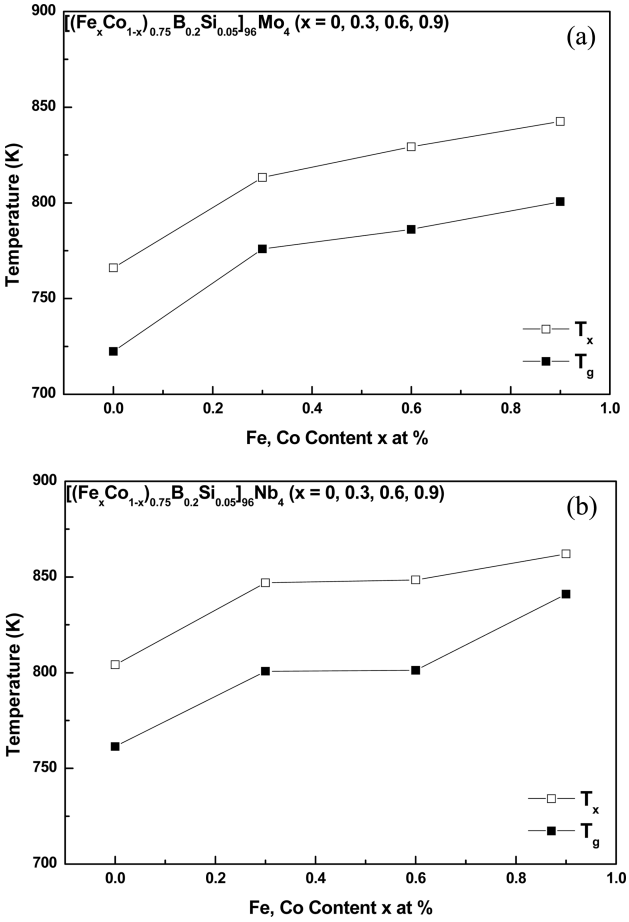

Fig. 1. DSC traces of (a) $[(Fe_xCo_{1-x})_{0.75}B_{0.2}Si_{0.05}]_{96}Mo_4$ (x = 0, 0.3, 0.6, 0.9) and (b) $[(Fe_xCo_{1-x})_{0.75}B_{0.2}Si_{0.05}]_{96}Nb_4$ (x = 0, 0.3, 0.6, 0.9) amorphous ribbons as a function of Fe, Co content.

3. Results and Discussion

The thermal properties of $[(Fe_xCo_{1-x})_{0.75}B_{0.2}Si_{0.05}]_{96}Mo_4$ (x = 0, 0.3, 0.6, 0.9 at. %) and $[(Fe_xCo_{1-x})_{0.75}B_{0.2}Si_{0.05}]_{96}Nb_4$ (x = 0, 0.3, 0.6, 0.9 at. %) were examined. The DSC traces of Fe-Co-B-Si-M (M = Mo and Nb) ribbon are shown in Fig. 1. The glass transition temperature (T_g) and crystallization temperature (T_x) of amorphous ribbons $[(Fe_xCo_{1-x})_{0.75}B_{0.2}Si_{0.05}]_{96}Mo_4$ (x = 0, 0.3, 0.6, 0.9 at. %) and $[(Fe_xCo_{1-x})_{0.75}B_{0.2}Si_{0.05}]_{96}Nb_4$ (x = 0, 0.3, 0.6, 0.9 at. %) were measured using differential scanning calorimetry (DSC). T_g and T_x represent the onset temperature of the glass transition temperature and the first crystallization exothermal event, respectively; and the value of the ($T_x - T_g$) is defined as supercooled liquid region ΔT_x. Thermal properties such as T_x, T_g and ΔT_x are listed in Table 1. The ΔT_x range of amorphous ribbons $[(Fe_xCo_{1-x})_{0.75}B_{0.2}Si_{0.05}]_{96}Mo_4$

Table 1. Thermal, mechanical and magnetic properties of $[(Fe_xCo_{1-x})_{0.75}B_{0.2}Si_{0.05}]_{96}Mo_4$ (x = 0, 0.3, 0.6, 0.9) and $[(Fe_xCo_{1-x})_{0.75}B_{0.2}Si_{0.05}]_{96}Nb_4$ (x = 0, 0.3, 0.6, 0.9) amorphous ribbons.

Alloys	Thermal properties			Mechanical properties			Magnetic properties	
	T_g (K)	T_x (K)	ΔT_x (K)	H (GPa)	H (Vickers)	E_r (GPa)	H_c (Oe)	M_s (emu/g)
$Co_{72}B_{19.2}Si_{4.8}Mo_4$	722.4	766.0	43.6	15.32	1418.45	151.4	0.14	79.84
$Fe_{21.6}Co_{50.4}B_{19.2}Si_{4.8}Mo_4$	775.9	813.3	37.4	14.05	1301.63	125.0	0.25	101.73
$Fe_{43.2}Co_{28.8}B_{19.2}Si_{4.8}Mo_4$	786.1	829.3	43.2	18.32	1694.42	268.5	0.11	142.63
$Fe_{64.8}Co_{7.2}B_{19.2}Si_{4.8}Mo_4$	800.6	842.5	41.9				0.15	128.03
$Co_{72}B_{19.2}Si_{4.8}Nb_4$	761.4	804.1	42.7				0.32	67.62
$Fe_{21.6}Co_{50.4}B_{19.2}Si_{4.8}Nb_4$	800.7	847.0	46.3	18.16	1682.01	137.4	0.31	109.23
$Fe_{43.2}Co_{28.8}B_{19.2}Si_{4.8}Nb_4$	801.2	848.5	47.3	15.04	1392.65	122.7	0.32	129.26
$Fe_{64.8}Co_{7.2}B_{19.2}Si_{4.8}Nb_4$	814.0	862.1	48.1				0.11	82.14

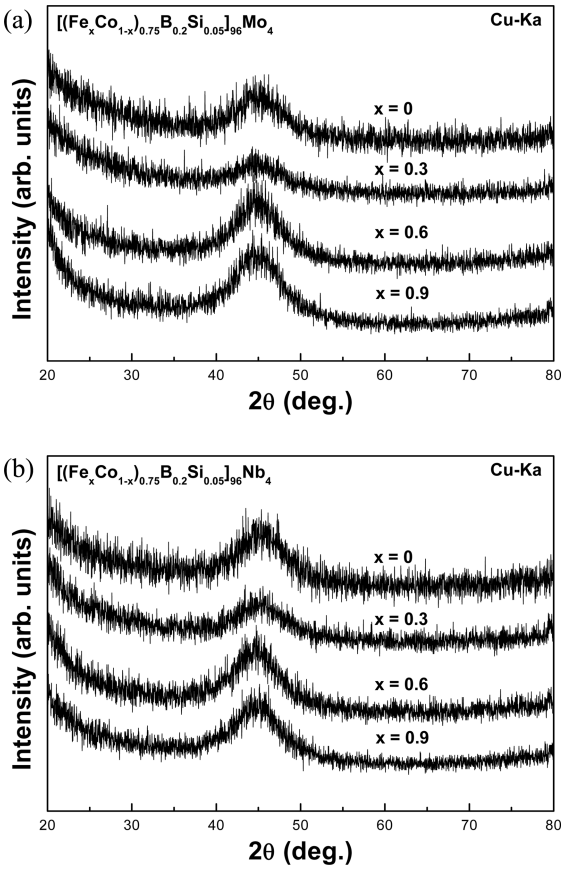

Fig. 2. XRD patterns of (a) $[(Fe_xCo_{1-x})_{0.75}B_{0.2}Si_{0.05}]_{96}Mo_4$ (x = 0, 0.3, 0.6, 0.9) and (b) $[(Fe_xCo_{1-x})_{0.75}B_{0.2}Si_{0.05}]_{96}Nb_4$ (x = 0, 0.3, 0.6, 0.9) amorphous ribbons.

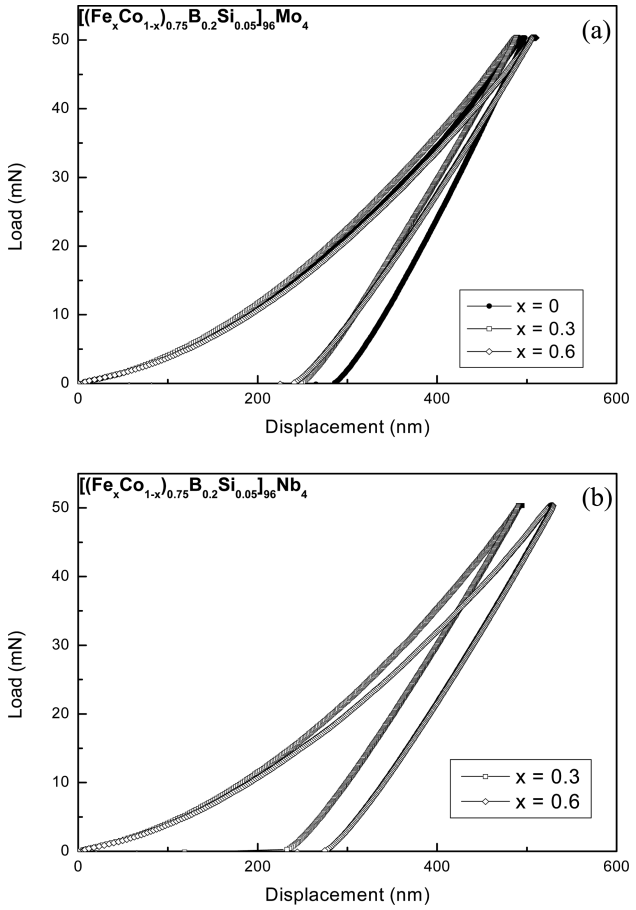

Fig. 3. Nano-indentation diagrams load (mN) obtained by applying symmetric triangle force pulses to the indenter of (a) $[(Fe_xCo_{1-x})_{0.75}B_{0.2}Si_{0.05}]_{96}Mo_4$ (x = 0, 0.3, 0.6) and (b) $[(Fe_xCo_{1-x})_{0.75}B_{0.2}Si_{0.05}]_{96}Nb_4$ (x = 0.3, 0.6) amorphous ribbons.

(x = 0, 0.3, 0.6, 0.9 at. %) was 37.4-43.6 K. According to the results, for ribbons of Fe-Co-B-Si-Mo with a larger proportion of Co than Fe, the T_g and T_x increase gradually up to 800.6 K and 842.5 K, respectively. Also, $Co_{72}B_{19.2}Si_{4.8}Mo_4$ (x = 0) has the largest ΔT_x. The ribbons of $[(Fe_xCo_{1-x})_{0.75}B_{0.2}Si_{0.05}]_{96}Nb_4$ (x = 0, 0.3, 0.6, 0.9 at. %) have ΔT_x in the range of 42.7-48.1 K. The T_g and T_x also increased gradually up to 814.0 K and 862.1 K, respectively; and $Fe_{64.8}Co_{7.2}B_{19.2}Si_{4.8}Nb_4$ (x = 0.9) has the largest ΔT_x. Comparing the results of thermal properties in FeCoBSiM systems, ribbons containing 4 at. % Nb are more thermally stable than ribbons containing 4 at. % Mo, as the FeCoBSiNb system has a wide supercooled liquid region (ΔT_x). Therefore, FeCoBSiNb system is more thermally stable than FeCoBSiMo system.

The X-ray diffraction patterns of $[(Fe_xCo_{1-x})_{0.75}B_{0.2}Si_{0.05}]_{96}Mo_4$ (x = 0, 0.3, 0.6, 0.9 at. %) and $[(Fe_xCo_{1-x})_{0.75}B_{0.2}Si_{0.05}]_{96}Nb_4$ (x = 0, 0.3, 0.6, 0.9 at. %) from melt-spun ribbons are shown in Fig. 2. These ribbons have a fully amorphous phase, as there are no sharp Bragg peaks and all diffraction curved lines show the typical broad halo pattern. The broad halo patterns indicate that these ribbons consist of a fully amorphous phase.

The mechanical properties of Fe-Co-B-Si-M amorphous ribbon samples were measured using the technique of nano-indentation. Nano-indentation is used in thin and ultra-thin films with small volumes [18]. Nanohardness (H), Vickers Hardness (H_v) and reduced elastic modules (E_r) of $[(Fe_xCo_{1-x})_{0.75}B_{0.2}Si_{0.05}]_{96}Mo_4$ (x = 0, 0.3, 0.6 at. %) and $[(Fe_xCo_{1-x})_{0.75}B_{0.2}Si_{0.05}]_{96}Nb_4$ (x = 0.3, 0.6 at. %) were tested by the nano-indentation technique (Table 1). Mechanical properties of $[(Fe_xCo_{1-x})_{0.75}B_{0.2}Si_{0.05}]_{96}Mo_4$ (x = 0.9 at. %) and $[(Fe_xCo_{1-x})_{0.75}B_{0.2}Si_{0.05}]_{96}Nb_4$ (x = 0, 0.9 at. %) could not be measured by nano-indentation, as the sample surfaces were slippery. The nanohardness (H) of Fe-Co-B-Si-Mo and Fe-Co-B-Si-Nb amorphous ribbons was in the range of 14.05-18.32 GPa and 15.04-18.16 GPa, respectively. The Vickers hardness (H_v) of Fe-Co-B-Si-Mo and Fe-Co-B-Si-Nb amorphous ribbons was in the range of 1301.63-1694.42 Vickers, respectively. The reduced

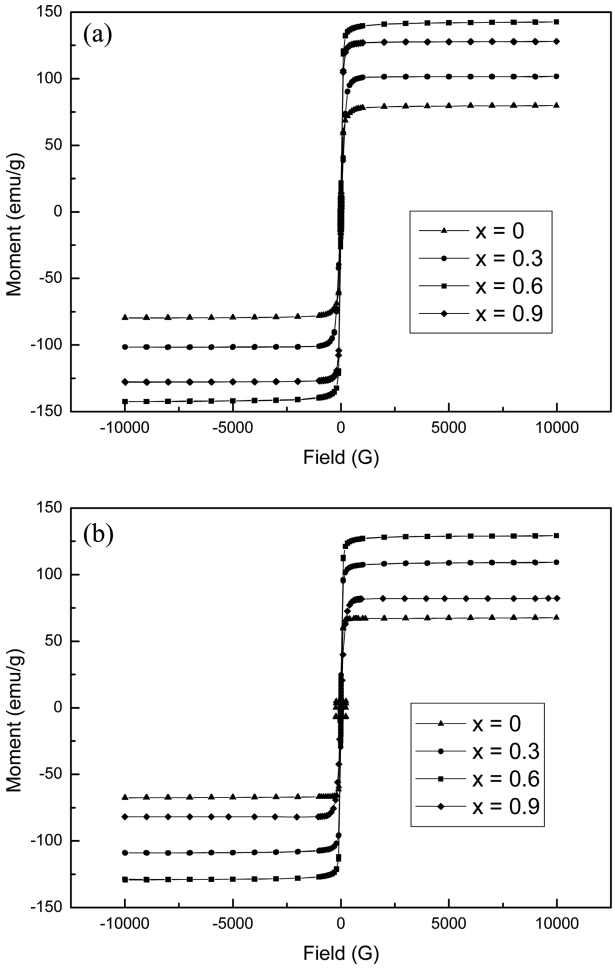

Fig. 4. Hysteresis loops of (a) $[(Fe_xCo_{1-x})_{0.75}B_{0.2}Si_{0.05}]_{96}Mo_4$ (x = 0, 0.3, 0.6, 0.9) and (b) $[(Fe_xCo_{1-x})_{0.75}B_{0.2}Si_{0.05}]_{96}Nb_4$ (x = 0, 0.3, 0.6, 0.9) amorphous ribbons.

elastic modulus (E) of Fe-Co-B-Si-Mo and Fe-Co-B-Si-Nb amorphous ribbons was in the range of 151.4-268.5 GPa and 122.7-137.4 GPa, respectively. The load-displacement (p-h) curves of $[(Fe_xCo_{1-x})_{0.75}B_{0.2}Si_{0.05}]_{96}Mo_4$ (x = 0, 0.3, 0.6 at. %) and $[(Fe_xCo_{1-x})_{0.75}B_{0.2}Si_{0.05}]_{96}Nb_4$ (x = 0.3, 0.6 at. %) are shown in Fig. 2.

Magnetic properties of amorphous ribbon samples were measured using VSM. The hysteresis M–H loop of the as-spun $[(Fe_xCo_{1-x})_{0.75}B_{0.2}Si_{0.05}]_{96}Mo_4$ (x = 0, 0.3, 0.6, 0.9 at. %) and $[(Fe_xCo_{1-x})_{0.75}B_{0.2}Si_{0.05}]_{96}Nb_4$ (x = 0, 0.3, 0.6, 0.9 at. %) is identified in Fig. 4. The Fe-Co-B-Si-Mo amorphous ribbons presented soft magnetic properties with a low coercive force (H_c) range of 3.89-4.64 Oe and high saturation magnetization (M_s) range of 79.84-142.63 emu/g. Also Fe-Co-B-Si-Nb amorphous ribbons exhibited soft magnetic properties with a low coercive force (H_c) range of 4.42-4.54 Oe and high saturation magnetization (M_s) range of 67.62-129.26 emu/g.

The amorphous ribbons of Fe-Co-B-Si-M (x = 0 at. %) exhibited the highest thermal stability with large supercooled liquid regions. Also, T_g, T_x and ΔT_x increased with increasing Fe content, in x = 0.3, 0.6, 0.9 at. %. The reasons for the Fe-based systems having a high GFA is that these systems satisfy the following empirical rules. First, the alloy system should have more than three elements, and the alloy system must contain elements with different atomic size ratios above 12% among the main constituent elements. FeCoBSiM alloys are multi-component systems, and they have a radius difference in the atomic size ratio above 12%. The radius change of main element is as follows: Nb (0.143 nm) > Mo (0.139 nm) > Co (0.125 nm) > Fe (0.124) nm. Also, Fe and Co have nearly the same atomic radii (0.125 nm, 0.124 nm), so that they may be substituted in a suitable proportion to make for proper magnetic properties. Second, elements should have negative heat in the mixing of their elements. These Fe-Co-B-Si-M amorphous ribbons alloys have high negative mixing enthalpies, so that they have high thermal stability. For example, the mixing enthalpies between Fe and B, Si, Mo or Nb atomic pairs are −11, −18, −2 and −16 kJ/mol, respectively; and the mixing enthalpy for B-Mo, B-Nb pairs are −39 kJ/mol and −19 kj/mol, respectively. The mixing enthalpy of Si-Mo and Si-Nb pairs are −39 kJ/mol and −18 kJ/mol, respectively. The addition of a small amount of Mo and Nb will have beneficial effects on the thermal stability and glass forming ability of amorphous alloys.

4. Conclusion

In conclusion, Fe-Co-B-Si-M systems were investigated by DSC, XRD, nano-indentation and VSM. These amorphous ribbons have a high GFA, and the addition of M may have beneficial effects on thermal stability. Alloy with 4 at. % of Nb has a higher GFA compared to an alloy with 4 at. % of Mo. Increasing the proportion of Fe in Fe-Co-B-Si-M amorphous ribbons tends to enlarge the supercooled liquid region, except for $[(Fe_xCo_{1-x)0.75}B_{0.2}Si_{0.05}]_{96}Mo_4$ and $[(Fe_xCo_{1-x)0.75}B_{0.2}Si_{0.05}]_{96}Nb_4$ at x = 0. Also, amorphous ribbons of $[(Fe_xCo_{1-x)0.75}B_{0.2}Si_{0.05}]_{96}Mo_4$ (x = 0, 0.3, 0.6, 0.9 at. %) and $[(Fe_xCo_{1-x)0.75}B_{0.2}Si_{0.05}]_{96}Mo_4$ (x = 0, 0.3, 0.6, 0.9 at. %) show soft-magnetic properties, with low coercive force (H_c) and high saturation magnetization (M_s).

Acknowledgments

The author is grateful to Ms. Soohyun Im (Sejong University) for her contributions.

References

[1] W. L. Johnson, MRS Bull. **24**, 42 (1999).
[2] W. Klement, R. H. Willens, and P. Duwez, Nature **187**, 869 (1960).
[3] Y. H. Liu, G. Wang, R. J. Wang, D. Q. Zhao, M. X. Pan, and W. H. Wang, Science **315**, 1385 (2007).
[4] A. Inoue, B. L. Shen, and C. T. Chang, Acta Mate. **52**, 4093 (2004).
[5] A. R. Yavari, J. J. Lewandowski, and J. Eckert, MRS Bull. **32**, 635 (2007).
[6] J. Eckert, M. Seidel, N. Schlorke, A. Kubler, and L. Schultz, Mater. Sci. Forum **235**, 23 (1997).
[7] B. L. Shen, A. Inoue, and C. T. Chang, Appl. Phys. Lett. **85**, 4911 (2004).
[8] C. T. Chang, B. L. Shen, and A. Inoue, Mater. Sci. Eng. A **449**, 239 (2007).
[9] S. J. Pang, T. Zhang, K. Asami, and A. Inoue, Acta Mater. **50**, 489 (2002).
[10] S. F. Guo, L. Liu, N. Li, and Y. Li, Scri. Mater. **62**, 329 (2010).
[11] A. Inoue and A. Makino, Nano. Mater. **9**, 403 (1997).
[12] A. Inoue, Mater. Sci. Eng. **304**, 1 (2001).
[13] R. B. Schwarz, T. D. Shen, V. Harms, and T. Lillo, J. Magn. Magn. Mater. **283**, 223 (2004).
[14] K. Hayashi, M. Hayakawa, Y. Ochiai, H. Matsuda, W. Ishikawa, and K. Aso, J. Appl. Phys. **61**, 2983 (1987).
[15] A. Datta and C. H. Smith, Rapidly Quenched Metals, vol. eds. S. Steeb and H. Warlimont, North-Holland, Amsterdam, Oxford, New York, Tokyo (1985), p. 1315.
[16] T. Komatsu, S. Sato, and K. Matusita, Acta. Mater. **34**, 1899 (1986).
[17] B. L. Shen, C. T. Chang, T. Kubota, and A. Inoue, J. Appl. Phys. **100**, 013515 (2006).
[18] N. Dwivedi, S. Kumar, and H. K. Malik, App. Surf. Sci. **257**, 9953 (2011).
[19] L. A. Deibler and K. O. Findley, J. Alloys Compd. **463**, 173 (2008).
[20] D. Pan, A. Inoue, T. Sakurai, and M. W. Chen, Proc. Natl. Acad. Sci. U.S.A. **105**, 14769 (2008).